IEEE/CSC & ESAS SUPERCONDUCTIVITY NEWS FORUM (global edition), January 2016.
EUCAS 2015 preprint 1A-LS-P-05.08. Submitted to *IEEE Trans. Appl. Supercond.* for possible publication.

Design of a 56 GJ Twin Solenoid & Dipoles Detector Magnet System for the Future Circular Collider

Matthias Mentink, Alexey Dudarev, Helder Filipe Pais Da Silva, Christophe Paul Berriaud, Gabriella Rolando, Rosalinde Pots, Benoit Cure, Andrea Gaddi, Vyacheslav Klyukhin, Hubert Gerwig, Udo Wagner, and Herman ten Kate

***Abstract*—An aggressive low mass and high stress design of a very large detector magnet assembly for the Future Circular Collider (FCC-hh), comprising a "Twin Solenoid" and two dipoles, is presented. The twin solenoid features two concentric solenoids. The inner solenoid provides 6 T over a free bore of 12 m and a length of 20 m, enclosing the inner particle trackers as well as electron and hadron calorimeters. The outer solenoid reduces the stray field of the inner solenoid and provides additional bending power for high-quality muon tracking. Dipoles are included providing 10 Tm of bending power in a 6 m mean free bore covering the forward directions for $\eta \geq 2.5$ particles. The overall length of this magnet assembly is 43 m.**

The presence of several separate magnets in the system presents a challenge in terms of forces and torques acting between them. A rigid support structure, part of the cold mass, holds the inner and outer solenoids of the twin solenoid in place. The dipoles are equipped with lateral coils so that the net force and torque are reduced to zero.

The second challenge is the substantial conductor and support structure mass used for containing the magnetic pressure. A doped aluminum stabilized and reinforced conductor is proposed allowing minimal overall mass of the system.

The result is a system comprising a 53 GJ twin solenoid, and two 1.5 GJ dipoles. The cold mass and vacuum vessel mass of the twin solenoid are 3.2 and 2.4 kt, respectively, and the dipole cold mass weighs 375 tons. Various properties of the magnet system are discussed such as magnetic, mechanical and thermal properties, quench behavior, and assembly.

***Index Terms*—FCC, detector magnet, twin solenoid, dipole**

I. Introduction

CERN has started the conceptual design of a Future Circular Collider (FCC-hh). In comparison to the Large Hadron Collider (LHC), the collision energy of FCC is 7 times higher, which means that new and much more powerful particle detectors for studying the collision products are needed. Various concepts are being studied, like a twin solenoid in combination with two dipoles and a classical iron-yoke-based solenoid.

The twin solenoid design features two concentric anti-series connected superconducting solenoids. The inner solenoid provides 6 T central field over a free bore of 12 m and a length of 20 m. The outer solenoid serves two purposes, which are to reduce the stray field of the twin solenoid to a level where magnetic-field-sensitive electronics and other services equipment may be placed within a reasonable distance of the detector magnet, and secondly to provide a magnetic field of about 2.8 T in between the two solenoids to facilitate high-quality muon tracking. The main advantage of using active shielding with a superconducting solenoid is that this system becomes comparatively light-weight in comparison to a CMS-like iron-shielded solenoid scaled-up for such a large detector. Regarding the twin solenoid a few versions exist with various conductor concepts and levels of stress and strain in the cold mass. There is clearly a trade-off between cold mass weight and strain. Here we prevent a version attempting to minimize the cold mass thereby accepting enhanced strain in the conductor. The details of the twin solenoid are discussed in section II.

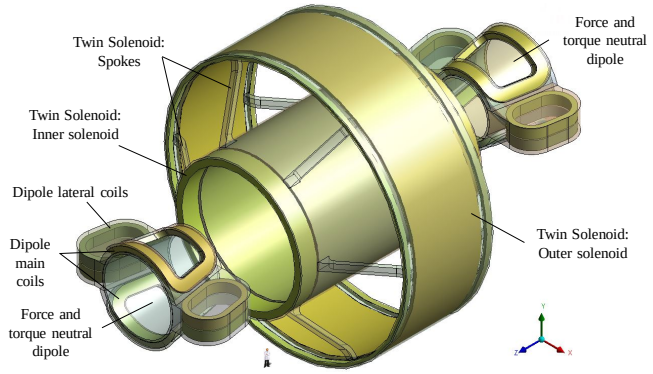

Fig. 1. Cold mass of the twin solenoid and dipoles. In this figure the support structure is made partially transparent to reveal the superconducting coils. The outer diameter and total assembly length is 27 and 43 m, respectively.

Particle tracking in the forward direction ($\eta \geq 2.5$) is facilitated through two dipoles (Fig. 1). Similar to the twin solenoid, the stray field of these dipoles is reduced through the use of lateral coils, which also perform the function of reducing the net force and torque on these dipoles to practically zero. Details of these dipoles are discussed in section III.

This paper covers a range of conceptual topics, including overall geometry, magnetic field and field integrals, mechanical and thermal properties, quench behavior, and assembly of the twin solenoid and dipoles.

Christophe Paul Berriaud is affiliated with CEA and the other authors are affiliated with CERN. All authors are affiliated with the FCC-hh Detector Magnets Working Group. The primary author (email: matthias.mentink@cern.ch) is with the ATLAS magnet group, Physics Department, CERN, 1217 Meyrin, Switzerland.

IEEE/CSC & ESAS SUPERCONDUCTIVITY NEWS FORUM (global edition), January 2016.
EUCAS 2015 preprint 1A-LS-P-05.08. Submitted to *IEEE Trans. Appl. Supercond.* for possible publication.

TABLE I
TWIN SOLENOID PROPERTIES

Stored energy	53 GJ	Conductor dim.	90×90 mm^2
Total mass	5.6 kt	I_c(4.6 K, B_{Peak})	420 kA
Conductor mass	2.3 kt	Supercond. (3 vol.%)	NbTi
Vac. vessel mass	2.4 kt	Matrix (3 vol.%)	Cu
Operating current	80 kA	Stabilizer (34 vol.%)	Al(-Ni)
Self-inductance	16.6 H	Jacket (60 vol.%)	Al-alloy
B_{Peak}	6.44 T	Energy extr. (1000 V)	30 %
Conductor length	102 km	Avg. T after quench	88 K

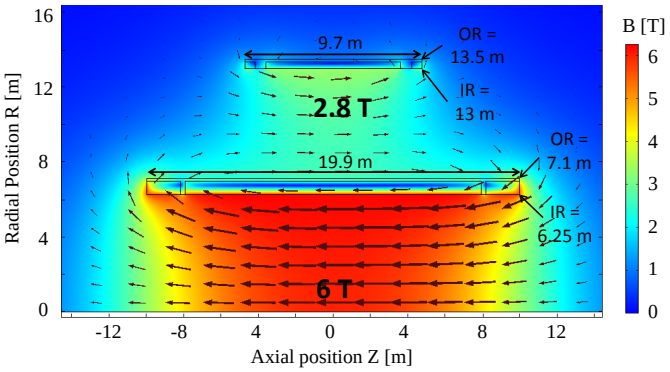

Fig. 2. Geometry of the twin solenoid cold mass, and magnetic field lines.

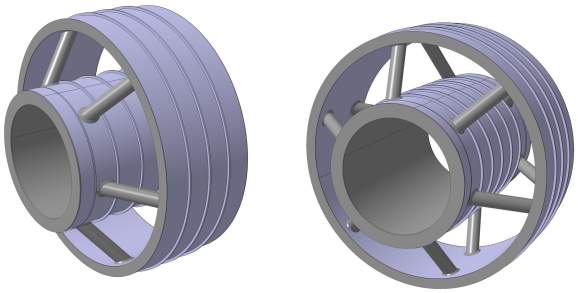

Fig. 3. Vacuum vessel of the twin solenoid surrounding the cold mass and comprising 2.4 kt of stainless steel.

II. TWIN SOLENOID DESIGN

A. Geometry

The cold mass consists of two support cylinders for the inner and outer solenoids, each holding in place three superconducting coil modules (Fig. 1, Table I). The separation into center coil and two edge coils ensures a proper mechanical connection between the coils and support structure during operation. The edge coils push radially outwards and axially inwards. The center coils push radially outwards and are compressed by the clamping force provided by the edge coils. Aluminum spacers are located between the edge coils and the center coil and are directly mechanically connected to the support cylinders. The inner and outer support structures are then mechanically linked by spokes which are part of the cold mass (Fig. 1).

For the sake of this design a conductor with dimensions of 90×90 mm^2 is taken. It comprises a high-strength jacket enclosing a core of 64 mm diameter which is filled with a cable of NbTi/Cu and aluminum strands. The jacket has a yield strength of 350 MPa at 4.5 K when using Al-6060-T6 [1] or even 700 MPa when using Al-7020.72 [2]. The operating current of this conductor is 80 kA (i.e. 9.8 A/mm^2 overall), so that a temperature margin of 1.5 K gives a critical current of 420 kA, and a composition of 3 vol.% NbTi [3], 3 vol.% Cu, 34 vol.% aluminum stabilizer and 60 vol.% doped aluminum. Note that conductor optimization is not the subject of this paper and a more detailed conductor investigation is to be published elsewhere [4].

With the assumed conductor geometry, the distribution of turns is as follows: 8×176 in the central coil of the inner solenoid, 8×20 for each of the edge coils in the inner solenoid, 4×80 in the central coil of the outer solenoid, and 4×6 for each of the edge coils in the outer solenoid. This requires a total conductor length of 102 km. The spacers in the inner and outer solenoid are 0.25 and 0.60 m wide, respectively.

The length of the outer solenoid cold mass is 9.7 m, about half the length of the inner solenoid (Fig. 2). This has a number of benefits. Firstly, this geometry matches well with the conductor dimensions by which the inner solenoid and outer solenoid have 8 and 4 layers, respectively. Secondly, as the projection of the twin solenoid in transverse direction to the axis is roughly spherical, the shaft diameter required for lowering the twin solenoid into the detector cave is minimized even when the outer solenoid is lowered as a single module. Thirdly, the magnetic field in between the solenoids at $\eta = 0$ is increased due to the more concentrated current in the outer solenoid, while still providing sufficient field integral at higher η. Fourthly, this geometry provides space for a support structure supporting the trackers, the calorimeters and the twin solenoid itself. The downside of this low length ratio is a somewhat increased stray field: The 5 mT stray field boundary is shaped like a peanut, with the magnitude dropping below 5 mT at R = 35 m at its widest point, R = 32 m at Z = 0 and Z = 57 m at R = 0.

The stored energy of the twin solenoid is 53 GJ, about 20 and 35 times higher than in CMS and ATLAS, respectively. Being stress-limited, the cold mass scales with the stored energy of the system, and a cold mass of several kt is unavoidable. To avoid assembly of many modules inside the detector cavern (assuming weight-limitations in the crane), emphasis in this design is on reducing the total system mass at the cost of a higher stress level in the coil windings. This leads to a total cold mass of 3.2 kt, with coils in the inner and outer solenoid weighing 1.6 kt and 0.7 kt, respectively. The support structures for the inner and outer solenoid each weighs 0.4 kt and the spokes weigh 90 tons in total.

The vacuum vessel (Fig. 3) consists of 2.4 kt of stainless steel, 304L and 304LN, of which 1.4 kt surrounds the inner solenoid. The entire cold mass of the inner and outer coils is suspended through two sets of tie rods to the end flanges of the inner coil cryostat. The inner bore of the vacuum vessel consists of 80 mm thick 304LN which is sufficiently strong to support the detector mass positioned in the bore tube of up

TABLE II
PEAK VON MISES STRESS IN THE TWIN SOLENOID UNDER VARIOUS CONDITIONS.

Condition	Coil σ_{Peak} [MPa]	Support σ_{Peak} [MPa]
Just gravity (G)	170	140
G + 50 mm axial misalignment	170	140
G + 50 mm off-axis misalignment	170	140
G + 1.2 G axial	170	170
2.2 G off-axis	170	140
G + 0.3° rotation	170	180

to 15 kt.

B. Magnetic field

Fig. 2 shows the orientation of the magnetic field. To provide bending power to the collision products originating at the center of the twin solenoid, a magnetic field component perpendicular to the particle trajectory is needed. Measures of the degree of bending power and the sagitta are given by the first and second integral of the perpendicular magnetic field respectively [8], following:

$$I_1 = \int_0^L B_\perp dl, \tag{1}$$

$$I_2 = \int_0^L \int_0^L B_\perp dl^2, \tag{2}$$

where $B_\perp$ is the magnetic field component perpendicular to the trajectory out of a particle emanating from the center of the twin solenoid and L is the distance to the center. The curvature of the particle trajectory is assumed negligible (i.e. particles with high momentum), so that it may be approximated with a straight line.

Fig. 4 shows the perpendicular magnetic field, field integral and double field integral of the magnetic field generated by the twin solenoid, respectively. The location of the inner solenoid at R = 6.25 - 7.1 m is clearly visible from the rapid drop in field magnitude. In general the maximum values in $B_\perp$ and I_1 drop with increasing η while the maximum value in I_2 rises. This is due to the increase in path-length with increasing η. However, there is a practical limit to the distance at which detectors can be placed away from the center of the twin solenoid, which is why dipoles are proposed that provide additional bending power for high-η charged particles.

C. Mechanical properties

Two types of mechanical simulations were performed: a three-dimensional linear simulation in which the entire magnet is assumed to be made from aluminum alloy in the elastic regime and in which the influence of various external factors (gravity, misalignment of the inner solenoid versus the outer solenoid, and seismic events) on the stress state of the magnet was investigated, and an axisymmetric non-linear simulation

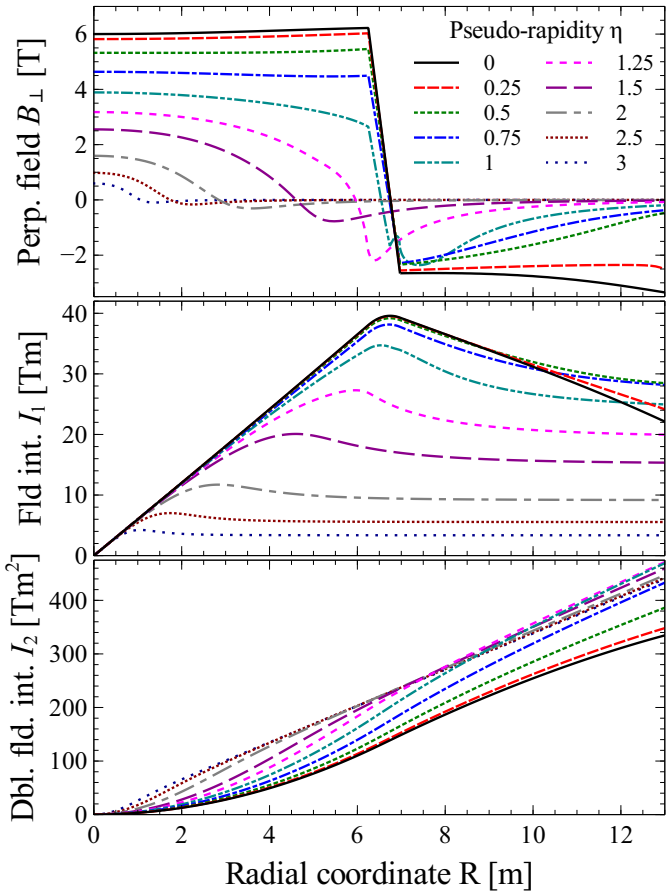

Fig. 4. Top: perpendicular magnetic field $B_\perp$ as a function of radial coordinate R at various pseudo-rapidities, only including the magnetic field of the twin solenoid. Middle: first field integral I_1. Bottom: second field integral I_2.

incorporating the conductor geometry, in which the local stress state in the conductor is evaluated.

The amount and shape of the support structures of the inner and outer solenoids were chosen in such a manner that the spokes, connecting the spacers in the inner and outer solenoid support structures, are placed under 0.02% compression when the magnet is at operating current. The spokes consist of high-strength aluminum alloy with a cross-section of 0.4×1.0 m^2 as they have to be sufficiently strong to handle gravity, seismic events, and forces resulting from misalignments. At nominal current and assuming minor misalignments the inner solenoid is radially forced to the center of the outer solenoid, forced outwards in the axial direction and tends to rotate to align the solenoidal magnetic field with that of the outer solenoid. The associated forces and torque are 100 MN/m from axial misalignment, 43 MN/m from off-axis misalignment, and 70 MNm/° from rotation misalignment. Here, the conductor properties are simplified and the support structure and windings are assumed to consist solely of aluminum alloy within the elastic limit. The current is homogeneously distributed in the conductor. Six cases are investigated in which the magnet is exposed to gravity, gravity + 50 mm axial misalignment, gravity + 50 mm off-axis misalignment, gravity + 1.2 G along the axial direction (where 1.2 G is used to approximate a

IEEE/CSC & ESAS SUPERCONDUCTIVITY NEWS FORUM (global edition), January 2016.
EUCAS 2015 preprint 1A-LS-P-05.08. Submitted to *IEEE Trans. Appl. Supercond.* for possible publication.

seismic event), 2.2 G along the off-axis direction, and finally gravity + 0.3° rotation of the inner solenoid with respect to the outer solenoid. The results of these calculations are shown in Table II. In all cases the peak coil stress is 170 MPa, while the peak stress in the support structure depends on the condition. In general the peak stress in the support structure occurs at the interfaces between the spokes and the support structure, while the peak stress in the overall support structure remains at 130 MPa.

In the non-linear axisymmetric simulation the core of the conductor is assumed dominated by aluminum 1100 with a Yield Strength of 40 MPa at 4.5 K [9], while the jacket consists of Al-6060-T6 alloy with a yield strength of about 350 MPa at 4.5 K [1]. The average von Mises stress in the jacket is then 185 MPa in the high-field region, with local maxima as high as 250 MPa. The peak tensile strain is as high as 0.25% in the stabilizer in the inner layer of the inner solenoid. Conversely, if the aluminum stabilizer is reinforced, for instance with nickel doping [2], [10], [11], [12], and stays within the elastic limit, then the peak stress is 150 MPa and the peak tensile strain reaches 0.19%.

D. Thermal properties and Quench behavior

The conductor operating temperature is calculated based on various assumptions. The outer surfaces of the support cylinders are assumed to be cooled indirectly to a temperature of 4.5 K. A 0.2 W/m^2 thermal radiation load is assumed [13]. 1 mm thick conductor-to-conductor and 2 mm thick conductor-to-ground resin-filled fiberglass insulations are used. Ignoring the ends of the coils where the temperature margin is substantially higher due to a lower magnetic field, the maximum temperature on the inner layer of the inner solenoid is below 4.6 K.

On quench detection multiple heaters are fired on the coil surfaces guaranteeing normal state in less than 10 s, which is short compared to the characteristic discharge time of about 400 s. In addition, quench back in the support cylinder provides significant backup to the quench heaters. With a residual resistivity ratio of 300, the amount of energy extraction by the dump resistor is dependent on the maximum allowed voltage drop over the coil, with 1000 V giving 30% extraction and an average coil windings temperature of 88 K.

E. Assembly scenario

Ideally, the degree of assembly in the cavern is kept to a minimum. The amount of modules to be lowered into the cavern and assembled there depends on the eventual weight of the system and weight limitations of the crane.

A split in two modules is possible by which the inner and outer solenoids are individually lowered and assembled in the cavern. In this case, each solenoid is produced following a process similar to the CMS solenoid [13], after which the vacuum vessels are temporarily secured to the cold masses at the cradles for the spokes. After lowering the modules into the cavern, the spokes and surrounding vacuum vessels are mechanically connected along with various other connections for conductor links. Finally the temporary supports between the vacuum vessels and the cradles can be removed step-by-step.

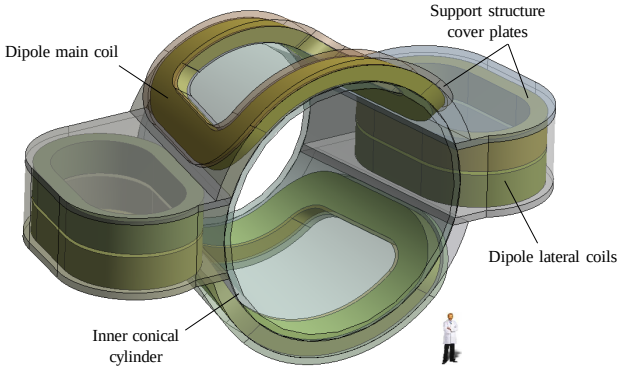

Fig. 5. Schematic representation of torque and force neutral conical dipoles. Here the support structure is made partially transparent to reveal the superconducting coils.

TABLE III
FORCE AND TORQUE NEUTRAL DIPOLE PROPERTIES

Stored energy	1.5 GJ	Cold mass	375 tons
Operating current	20 kA	Conductor mass	138 tons
B_{Peak}	6.0 T	Conductor length	37 km
Self-inductance	7.5 H	Mean free bore	6 m
Conductor peak stress	70 MPa	Field integral	10 Tm

III. FORCE AND TORQUE NEUTRAL DIPOLES

A. Geometry

The geometry of the dipole magnets is shown in Fig. 5. The dipoles are approximately 6 m long and are located at Z = 15 m. The free bore is sufficiently large to allow particles at η = 2.5 to pass through, giving a mean free bore of approximately 6 m.

The combination of main and lateral coils is chosen to both reduce the stray field, such as in the R3B magnet system [15], and to warrant practically zero net force and torque in the dipoles in a manner that is similar to the AMS superconducting magnet [16]. Removal of the lateral coils would result in a net force of 23 MN in the y direction and a net torque of 170 MNm, which would represent a severe complication for the cold-to-room-temperature support structure.

The stored energy per dipole within the background magnetic field of the twin solenoid is 1.5 GJ. Roughly two-thirds of the energy is stored in the magnetic field generated by the lateral coils.

A conduction-cooled aluminum-stabilized NbTi conductor is used with a current density of 14.6 A/mm^2. An operating current of 20 kA gives a self-inductance of 7.5 H, a cross-section of 1.4×10^{-3} m^2 and a total conductor length of 37 km per dipole.

B. Magnetic field

The peak magnetic field on the dipole conductor is 6.0 T, both for the main and lateral dipole coils.

IEEE/CSC & ESAS SUPERCONDUCTIVITY NEWS FORUM (global edition), January 2016.
EUCAS 2015 preprint 1A-LS-P-05.08. Submitted to *IEEE Trans. Appl. Supercond.* for possible publication.

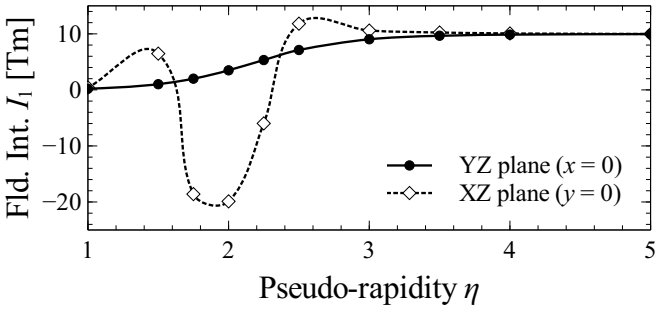

Fig. 6. Field integral I_1 of the dipoles, where the magnetic field contribution of the twin solenoid is not included.

The field integral of the dipole is more complicated than that of the twin solenoid, due to the lack of radial symmetry. In Fig. 6 it is given as a function of η over the XZ and the XY plane. Over the YZ plane the field integral is roughly constant at 10 Tm in the range η = 3 - ∞, and decreases with decreasing η. For the XZ plane, however, the magnetic field orientation in the lateral coils is opposite to that in the center, so that the field integral is initially positive for high η, then negative at $\eta \approx 2$, and then once again positive for lower η. On average, the field integral is 10 Tm for $\eta \geq 2.5$.

C. Mechanical properties and assembly

The 1 T stray field of the twin solenoid on the dipole conductor is significant (while the dipole stray field on the twin solenoid is below 25 mT). Thus, both magnitude and direction of forces inside the dipoles depend not only on the current in the dipoles but also on the current in the twin solenoid which means that the conductor needs to be tightly constrained to prevent possible movement.

For the assembly scenario, a 100 mm thick inner conical cylinder provides mechanical support. Side supports for the main dipole coils and support structures for the lateral coils are fixed onto this cone. The superconducting coils are wound and impregnated on mandrels and then transferred to the support structure. The inner support structure for the coils is then placed and cover plates are bolted on. Similar to the procedure utilized for the ATLAS barrel toroid coils [17], bladders may be used between the coil windows and the support structure, for the purpose of mechanically and thermally fixing the coils to the support structure while reducing the risk of quenches due to local cracking of the epoxy.

In this preliminary design, the cold mass consists of 375 tons of aluminum(-alloy), of which about one third is in the conductor. The peak Von Mises stress in the conductor is about 70 MPa. The peak stress in the support structure is 100 MPa, with peak stresses located at the interfaces between main and lateral support structures.

IV. Discussion

The combination of two-dimensional axisymmetric mechanical analyses, performed with COMSOL Multiphysics, and three-dimension mechanical analyses, performed with ANSYS Simulation Technology, provides an opportunity for consistency checks. In a one-to-one comparison the two-dimensional simulation indicates a peak stress of 150 MPa in the coil windings, while the three-dimensional simulation indicates a peak stress of 170 MPa, so that a more accurate overall value is 160±10 MPa. An issue with the three-dimensional analysis is that for the same meshing density the computational effort vastly exceeds that of the two-dimensional analysis, so that a trade-off between computational effort and meshing density is unavoidable. As such, the result from the three-dimensional analysis is likely somewhat pessimistic.

In this paper a high-stress high-strain approach is taken, in which the stored energy density of 16.6 kJ/kg exceeds a more conservative 12.2 kJ/kg such as used for the Compact Muon Solenoid [13] and is very high for a detector magnet. Opting for such a design provides clear advantages, such as a lower total stored energy, more available space for trackers and calorimeters, and a reduction in the amount of module assembly in the detector cavern for a given peak crane load. A detailed investigation is required to determine whether such an approach is feasible with regards to the conductor. Some issues that may prove problematic are the fabrication of high-strength joints and strain-cycling in the aluminum stabilizer, which could impact the RRR and thus the stability of the conductor. Previous research on nickel-doped aluminum-stabilized conductors [2], [10], [11], [12] has led to proposed conductors with effective yield strengths as high as 420 MPa [2] and a practical demonstration in the ATLAS solenoid conductor [14]. This technology may prove suitable for this high stress approach. In summary, a trade-off exists between various aspects of the design so that all possibilities should be explored to determine the optimal configuration. If it is determined that the level of stress and strain is overly challenging then the design may be adapted by adding additional aluminum alloy and thus increasing the overall cold mass.

V. Conclusion

An innovative design of a twin solenoid and two associated dipoles is presented, featuring full pseudo-rapidity coverage, with 36 Tm in the free bore at η = 0 and 10 Tm at $\eta = \infty$, in addition to high quality muon tracking. The twin solenoid comprises two concentric solenoids, where the inner bore provides 6 T over a 12 m free bore and the outer solenoid provides shielding and a 2.8 T magnetic field for muon tracking in the space in between the concentric solenoids. For the twin solenoid the preliminary design is targeted for minimum coil mass, while accepting higher stress and strain levels. The cold mass and vacuum vessel mass are 3.2 and 2.4 kt respectively, with a total stored magnetic energy of 53 GJ. To provide 10 Tm of bending power for $\eta \geq 2.5$ particles, two 1.5 GJ dipoles with 6 m mean free bores are proposed that are made force and torque neutral by using lateral coils. The cold mass of each dipole weighs 375 tons. The overall design has been discussed in terms of magnetic, thermal, and mechanical properties as well as assembly.

REFERENCES

[1] R. Heller, and the Wendelstein 7-X Technical Group, "Superconductor for the Coils of the Modular Stellarator Wendelstein 7-X", IEEE Trans. Magn. 30, p. 2383 (1994).
[2] S. Sgobba, "Options for yield strength enhancement of Al-stabilized superconductors", presentation at the ILC/CLIC Magnet Workshop, (2010).
[3] G. Sabbi, and P. Bauer, "Critical Current Parametrization and Short Sample Limit Calculation for the LHC IR Quadrupole Magnets", FNAL TD notes, TD-0-007 (1999).
[4] C. B. Berriaud *et al.*, "Preliminary conductor layouts for the detectors of the Future Circular Collider", to be published at MT24, (2015).
[5] D. Bessette, L. Bottura, A. Devred, N. Mitchell, K. Okuna, Y. Nunoya, C. Sborchia, Y. Takahashi, A. Verweij, A. Vostner, R. Zanino, and E. Zapretilina, "Test Results From the PF Conductor Insert Coil and Implications for the ITER PF System", IEEE Trans. Appl. Supercond. 19, p. 1525 (2009).
[6] V. I. Bondarenko, B. I. Egorov, Y. A.Klimchenko, O. A. Kovalchuck, E. L. Marushin, A. A. Mednikov, I. Y. Rodin, and V. M. Yarota, "Technology and Tooling for Manufacture Low-Ohm Electrical Joints for the ITER PF1 Coil", IEEE Trans. Appl. Supercond. 23, p. 4201605 (2013).
[7] J. Qin, Y. Wu, B. Liu, H. Liu, M. Yu, F. Long, F. Liu, Z. Wei, T. Xue, C. Su, K. Wang, S. Liu, and H. Li, "Manufacturing of ITER PF5 and CC Sample Conductors", IEEE Trans. Appl. Supercond. 24, p. 4202905 (2014).
[8] V. I. Klyukhin, A. Poppleton, and J. Schmitz, "Field Integrals for the ATLAS tracking volume", ATLAS internal note INDET-NO-023 (1993).
[9] Matweb material property data, "Properties of Aluminum 1100", www.matweb.com.
[10] K. Wada, S. Meguro, H. Sakamoto, A. Yamamoto, and Y. Makida, "High-strength and High-RRR Al-Ni Alloy for Aluminum-Stabilized Superconductor", IEEE Trans. on Appl. Supercond. 10, p. 1012 (2000).
[11] A. Yamamoto, Y. Makida, K. Tanaka, Y. Doi, T. Kondo, K. Wada, and S. Meguro, "Development towards ultra-thin superconducting solenoid magnets for high energy particle detectors", Nuc. Ph. B 78, pp. 565-570 (1999).
[12] S. Langeslag, B. Cure, S. Sgobba, A. Dudarev, and H. H. J. ten Kate, "Characterization of a Large Size Co-Extruded Al-Ni Stabilized Nb-Ti Superconducting Cable for Future Detector Magnets", IEEE Trans. on Appl. Supercond. 23, p. 4500504 (2013).
[13] CMS Collaboration, "CMS, the Magnet Project", Technical Design Report (1997).
[14] A. Yamamoto, T. Kondo, Y. Doi, Y. Maki, T. Tanaka, T. Haruyama, H. Yamaoka, H. H. J. ten Kate, L. Bjorset, K. Wada, S. Meguro, J. S. H. Ross, and K. D. Smith, "Design and Development of the ATLAS Central Solenoid Magnet", IEEE Trans. on Appl. Supercond. 9, pp. 852-855 (1999).
[15] B. Gastineau, C. Pes, and J. Ducret, "Comparison Between Active and Passive Shielding Designs for a Large Acceptance Superconducting Dipole Magnet", IEEE Trans. on Appl. Supercond. 16, p. 485 (2006).
[16] B. Blau, S. M. Harrison, H. Hofer, S. R. Milward, J. S. H. Ross, S. C. C. Ting, J. Ulbright, G. Viertel, "The Superconducting Magnet of AMS-02", Nuc. Phys. B. 113, pp. 125-132 (2002).
[17] J. Rey, M. Arnaud, C. Berriaud, R. Berthier, S. Cazaux, A. Dudarev, M. Humeau, R. Leboeuf, J. Gourdin, C. Mayri, C. Pes, H. ten Kate, and P. Vedrive, "Cold Mass Integration of the ATLAS Barrel Toroid Magnets at CERN", IEEE Trans. on Appl. Supercond. 16, p. 553 (2006).